Effect of driving frequency on the electron energy distribution function and electron-sheath interaction in a low pressure capacitively coupled plasmas

S. Sharma[1], N. Sirse[2], P. K. Kaw[1], M. M. Turner[2] and A. R. Ellingboe[2]

[1]Institute for Plasma Research (IPR), Gandhinagar-382428, India

[2] School of Physical Sciences *and* NCPST, Dublin City University, Dublin 9, Ireland

By using a self-consistent particle-in-cell simulation we investigated the effect of driving frequency (27.12–70 MHz) on the electron energy distribution function (EEDF) and electron-sheath interaction in a low pressure (5 mTorr) capacitively coupled Ar discharge for a fixed discharge voltage. We observed a mode transition with driving frequency, changing the shape of EEDF from a strongly bi-Maxwellian at a driving frequency of 27.12 MHz, to a convex type distribution at an intermediate frequency, 50 MHz, and finally becomes a weak bi-Maxwellian at a higher driving frequency i.e. above 50 MHz. The transition is caused by the electric field transients which is of the order of electron plasma frequency caused by the energetic 'beams' of electrons ejected from near the sheath edge. Below the transition frequency, 50 MHz, these high energy electrons redistributes their energy with low energy electrons thereby increasing the effective electron temperature in the plasma, whereas, the plasma density remains nearly-constant. Above the transition frequency high-energy electrons are confined between opposite sheaths which increases the ionization probability and therefore the plasma density increases drastically.

For many decades capacitively coupled plasma (CCP) excited at 13.56 MHz driving frequency have been utilized in the semiconductor processing industry for thin film deposition and plasma etching application. Presently, great interest is focused towards the excitation of CCP by frequencies up to few tens of MHz or even higher. This range is used in order to achieve enhanced plasma processing rates with lower damage to the substrate over a large-area wafer[1-2]. A CCP operated in the very high frequency (VHF) band, 30-300 MHz, produces higher plasma density due to an increase in the discharge current for a given discharge power and lower DC self-bias, thus achieving high-rate, low-damage processing, in contrast with low frequency plasma excitation.

Along with the plasma density and temperature, the plasma process is also affected by the radical densities which are determined by the Electron Energy Distribution Function (EEDF) i.e. the electron population above the threshold energy which causes electron-impact dissociation of gas molecules. Therefore, controlling the EEDF is crucial to improve and optimize the plasma processing rates. Previous experimental studies have shown a significant change in the EEDF with a change in the driving frequency[3-6]. Sugai et al.[3-6] showed that, depending on the gas pressure, a bi-Maxwellian (Maxwellian for non-Ramsauer gases) or convex type EEDF is observed at 13.56 MHz driving frequency, whereas the VHF plasma excitation mostly exhibits a bi-Maxwellian EEDF irrespective of gas pressure or type of gas (Ramsauer or non-Ramsauer). This is due to the enhanced stochastic heating at VHF excited CCP. In contrast to the experimental results, the simulation studies at 100 mTorr for direct comparison to the experimental work (Sugai et al.[3]) did not reproduce the measured change in EEDF[7].

In this letter, we investigate the effect of driving frequency (27.12-70 MHz) on the EEDF and electron sheath interaction in a low pressure (5 mTorr) CCP discharge using self-consistent particle-in-cell/ Monte-Carle collision (PIC/MCC) simulations. The PIC/MCC technique enables detailed investigation of power absorption by the plasma currents in the self-consistent electric fields (both instantaneous J.E and time averaged <J.E>). The simulation study is performed in an argon plasma at a constant discharge voltage (100 V). We observe a transition in EEDF from a strongly bi-Maxwellian distribution at 27 MHz driving frequency to a convex type distribution at an intermediate frequency (50MHz) and then finally a weak bi-Maxwellian distribution at higher frequencies (above 50 MHz). This transition is mainly due to the generation of energetic electrons from near the sheath edge which transfer energy to the bulk electrons and change the shape of the EEDF from strongly bi-Maxwellian to convex. Above a critical transition frequency (50 MHz), these high energy electrons are trapped between two sheaths, which increases the ionization probability. As a result the population of low energy electrons increases at a much faster rate compared to the high energy electrons which turn the EEDF into weakly bi-Maxwellian. Up to the transition frequency, the time-average electron density remains nearly-constant and the effective electron temperature increases two-fold, whereas, above the transition frequency the electron density increases rapidly and the effective electron temperature decreases. Below the transition frequency we observe positive <J.E> in the sheath with a small negative <J.E> across the center of the discharge, as is typically seen in previous PIC modeling. In contrast,

above the transition frequency there is a region adjacent to the sheath with strong negative <J.E> (electron cooling) with a positive <J.E> 'bump' in the middle of the discharge.

The present simulation technique is based on Particle-in-Cell/Monte Carlo collision (PIC/MCC) methods[8-9]. The PIC simulation provides the full kinetic information about the plasma like interaction of electrons with oscillating sheaths and includes the trajectories and loss of kinetic energy due to electron absorption at the walls etc. In the present research work, we have used well-tested 1D3V, self-consistent, electrostatic, PIC code developed at Dublin City University, Ireland[10]. Here the electron-neutral (elastic, inelastic and ionization) and ion-neutral (elastic, inelastic and charge exchange) collisions are considered for all set of simulations. The electrode gap is 3.2 cm and the operating pressure is 5 mTorr for all cases. The simulation region (3.2 cm electrode gap) is divided into 512 number of grids and number of particles per cell is 100 for all set of simulations. The time step has been chosen of the order of 10^{-11} s. We assume that electrodes are planar and parallel to each other with infinite dimension. We also ignored secondary electron emission and the electrodes are perfectly absorbing for both electrons and ions. One of the electrodes is grounded while an RF voltage having the following waveform drives the other one:

$$V_{rf}(t) = V_0 \sin(2\pi f_{rf} t + \phi) \qquad (1)$$

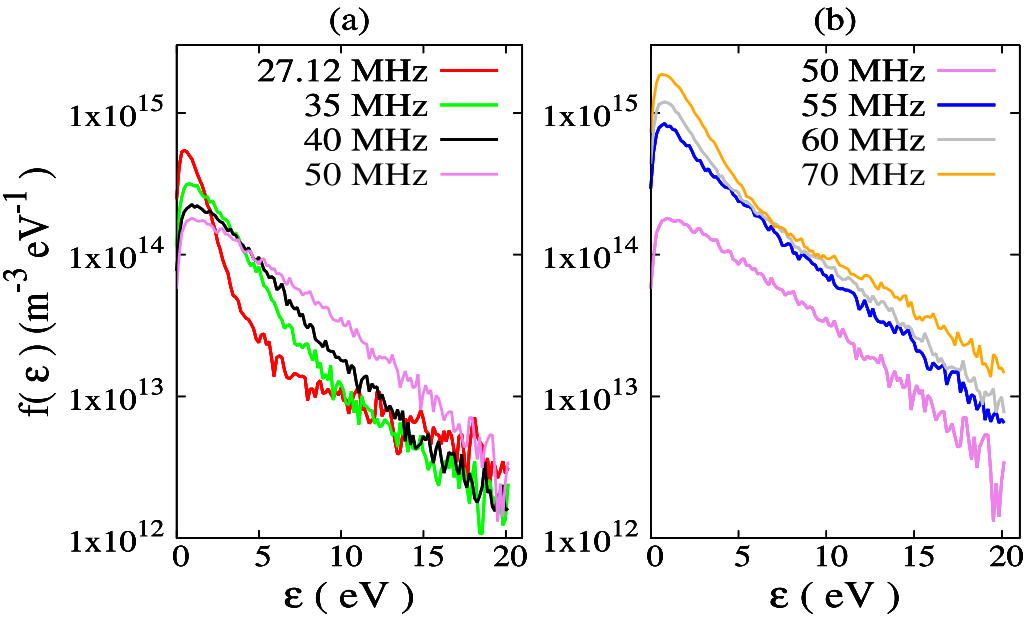

FIG. 1. Electron energy distribution functions at the centre of the discharge for a constant discharge voltage, 100V, and for different driving frequencies a) 27.12 MHz - 50 MHz b) 55 MHz – 70 MHz.

Figure 1 (a) and (b) shows the electron energy distribution function (EEDF) at the centre of the discharge for a constant discharge voltage, 100 Volts, and for various driving frequencies from 27.12 - 70 MHz. As displayed in figure 1 (a), at a frequency of 27.12 MHz the EEDF is strongly bi-Maxwellian with a large population (~89%) of low energy electrons (~1eV) and the remaining electrons in the high energy tail of ~10 eV. As driving frequency increases, from 27.12 MHz to 50 MHz, the low energy electron population decreases and the population of high energy electrons increases. The two-temperature form of EEDF turns into a convex type EEDF. At 50 MHz driving frequency, the simulated EEDF is fitted according to the equation, $A\exp\left(-\frac{E^r}{B}\right)$, Where E is the electron energy and A and B are constants. The simulated curved is best fit to a power function with an exponent, $r \sim 1.4$, and therefore called it as "convex type EEDF". With a further rise in driving frequency, i.e. above 50 MHz, the population of both low energy (80-85% at 70 MHz) and high energy (15-20% at 70 MHz) electrons increases (figure 1 (b)), however, the low energy electrons populate at a much faster rate when compared to high energy tail electrons and therefore the EEDF becomes a bi-Maxwellian.

Figure 2 plots the time averaged electron density at the centre of the discharge and the effective electron temperature (T_{eff})

$$T_{\text{eff}} = (2/3)\int \varepsilon F(\varepsilon)d\varepsilon \,/\, \int F(\varepsilon)d\varepsilon \qquad (2)$$

Where ε is the electron energy and $F(\varepsilon)$ is the self –consistent EEDF from the simulation. For the low pressure (5 mTorr) and small plasma gap (3.2 cm) the pre-sheath extends to the centre of the discharge, so the density in Figure 2 represents the peak density in the system. The peak plasma density remains nearly-constant up to 50 MHz. In contrast the effective electron temperature increases by two-fold i.e. from 1.6 eV at 27.12 MHz to 3.2 eV at 50 MHz. Above 50 MHz, the electron density increases sharply, from $1.2\text{x}10^{15}$ m^{-3} at 50 MHz to $4.5\text{x}10^{15}$ m^{-3} at 70MHz, and the T_{eff} drops back to 2.2 eV which is still higher in comparison to 27.12 MHz plasma excitation.

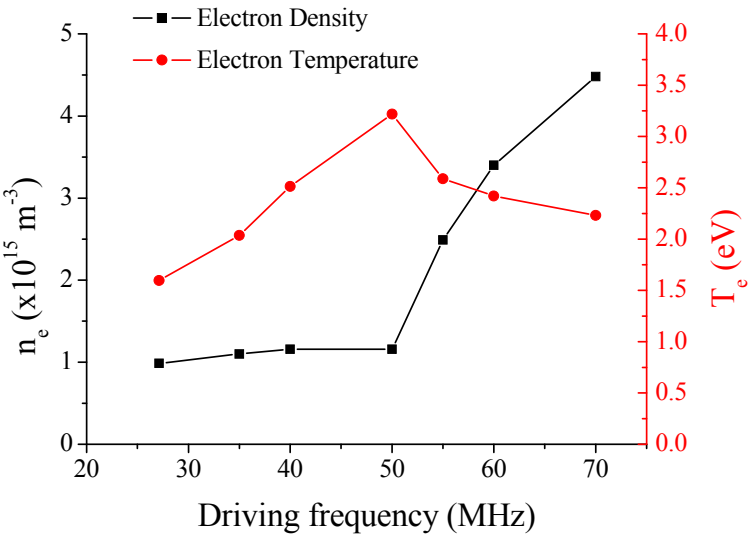

FIG. 2. Electron density and effective electron temperature versus driving frequency at the centre of the discharge for constant driving voltage, 100V.

The results clearly show a transition with frequency, which occurs between 50 MHz and 55 MHz in this specific case. Below the transition frequency the electron density remains nearly-constant with changing driving frequency and the shape of the EEDF changes from two-temperature Maxwellian to a convex type EEDF. Above the transition frequency the electron density increases sharply and the shape of the EEDF becomes a bi-Maxwellian, and the effective electron temperature decreases. This transformation leads to a partition of the power deposited into various inelastic and ionizing collisions. In this particular case, we observed a change in the inelastic collision rate from 0.84×10^{22} $m^{-3}s^{-1}$ at 27.12 MHz to 1.91×10^{22} $m^{-3}s^{-1}$ at 50MHz, whereas, the ionizing collisional rate is nearly-constant at ~1.5-2×10^{20} $m^{-3}s^{-1}$ up to 50 MHz. Above the transition frequency both inelastic and ionizing collision rates increase rapidly. In argon plasma this does not affect the mix of chemical species, however, in molecular gas this will substantially change the plasma and gas-phase chemistry. In the molecular gases there may be different EEDF is expected, however, we believe that the separation of power deposited into various inelastic and ionizing processes due to heating mode transition observed in present simulation results could lead to a control over dissociation and ionization of gas molecules (in molecular gases), and therefore a change in the ion to neutral flux is expected.

The strong bi-Maxwellian behavior of EEDF at a driving frequency of 27.12 MHz is on the one hand due to the long mean free path of low energy electrons of Ramsauer gases (Ar), which oscillate without collisions in the bulk and are unable to gain energy from the sheath

because of the presence of an ambipolar potential. On the other hand the high energy electrons can overcome the presence of ambipolar fields and are strongly heated by interaction with sheath electric fields[11].

As driving frequency increases the electric field from the sheath starts to penetrate into the bulk plasma. This is shown in Figure 3, in this figure the spatio-temporal evolution of the electric field is plotted for 4 different driving frequencies and for last 2 rf cycles of the simulation. As shown in Figure 3, (a) at 27.12 MHz the electric field is mostly confined in the sheath region, whereas at a driving frequency of 50 MHz, Figure 3 (b), there is significant electric field in the bulk plasma. The electric field in the bulk arises due to the electric field transients excited by high energy electrons coming from the sheath edge[12-14]. At low applied voltages ($|e\varphi(x)|/T_e<<1$) these transients act as linear excitations and phase mix in distance of order $v_{\text{th}}/\omega_{\text{rf}}$[15-17] where v_{th} is electron thermal velocity defined as $v_{\text{th}} = \sqrt{2T_e/m_e}$. At higher applied voltages ($|e\varphi(x)|/T_e>>1$), including the 100V sheath region in the present simulation, nonlinear processes changing the EEDF become important. These processes carry out an energy redistribution by transferring energy from high energy electrons to the bulk electrons and generates the observed convex type EEDF, causing a 2 fold increase in effective electron temperature for a driving frequency up to 50 MHz (Figure 1 (a)).

Above the transition frequency, Figure 3 (c) and (d), we observe a substantial high-frequency oscillation in the electric field at the sheath/bulk boundary. This can only be caused by directed electron flow from the bulk plasma into the sheath region changing the instantaneous sheath-edge position. These directed electron flows penetrate into the sheath field where they are reflected on an electron-quiver time-frame, and ejected back into the plasma. Depending on the phase of the sheath the ejected electrons gain/lose energy due to the time variation of the sheath voltage; The sheath-edge modulation is greatest during the sheath expansion phase (fig 3(d) left-side 3-10ns, right-side 10-18ns) thus net electron heating will occur. Concurrent with the onset of the transients in the sheath edge position are localized transients in electric field in the bulk plasma. These fields polarize the plasma causing spatio-temporal bunching of the high energy electrons directed towards the sheath, which in-turn enhances the sheath modulation. In this manner an initial perturbation in the high-energy electrons drives a self-sustaining electric field oscillation in the bulk plasma[15] which is roughly of the order of electron plasma frequency in this case (at 70 MHz, $f_{pe} = \sqrt{n_e e^2/\varepsilon_0 m}/(2\pi)$ = 634 MHz which is nearly 9 times of driving frequency).

The large perturbations in sheath-edge position during the expansion phase of the sheath give evidence of reflection of the high energy electrons back into the plasma. These electrons have energy greater than the ionization threshold (15.76 eV) enhancing the high-energy portion of the EEDF, Figure 1. This, in-turn, increases the ionization rate and the low-energy electron population which is trapped within the ambipolar electric field. This drives the transition to the bi-Maxwellian electron distribution and the reduction in the effective electron temperature. A similar, rapid rise in the electron density above a certain transition frequency is observed by Wilczek et al[14] in a narrow gap (1.5 cm) CCP for a gas pressure of 9.75 mTorr. At higher driving frequencies their results showed that the fast electrons are effectively confined between opposing sheaths.

We believe the transition is caused by the deep penetration of the non-linear transients into the bulk plasma which is getting stronger as driving frequency increases. In the linear case, the phase mixing length of these transient is $v_{\mathrm{th}}/\omega_{\mathrm{rf}}$[15-17], whereas, in the non-linear regime (which is the present case) the penetration of non-linear transients is complex and may depend on various other factors. A semi or full analytical model describing the on-set of the non-linear transients and the penetration depth of the high frequency oscillations is still under investigation.

Figure 4 plots the phase-averaged heating <J.E>. Below the transition frequency electron heating occurs mostly in the vicinity of the sheath edge, and the electron cooling i.e. negative <J.E>, in the bulk plasma (Figure 4 inset) which increases with frequency[15,18]. The electron cooling in the bulk results from an electric field in the bulk acting in opposition to the sheath-formed fast electrons, as well as phase-mixing between bulk electrons and tail electrons. Above the transition frequency the sheath heating moves closer to the plasmas boundary as the sheath-width decreases. The electron heating near the sheath edge continues to increase with the driving frequency, and in addition to this, an additional positive <J.E> is observed in the center of the discharge (Fig. 4 inset, at 60 and 70 MHz) plasma above the transition frequency. Physically this phenomenon may be explained as follows: the disturbances at the plasma-sheath boundary inject pulses of hot electrons into the bulk plasma. In the absence of electric fields, these pulses propagate into the bulk and produce some electron current density there that may be more or less than the total current density at the electrode. Since the current must be conserved, the electric field must adjust itself to produce the right current in the bulk. This could lead to an electric field of both sign, and hence positive or negative bulk heating. As one changes the frequency, the phase of these

pulses of hot electrons relative to total current in the bulk presumably changes. Hence, one might expect to find changes in the sign of the bulk heating as a function of frequency. Adjacent to the positive <J.E> in the sheath edge is a region of strong electron cooling, which arises from the reflected, bunched electrons interacting with the bulk plasma. We believe this provides the energy to form the plasma polarization electric field and the oscillations within the bulk plasma.

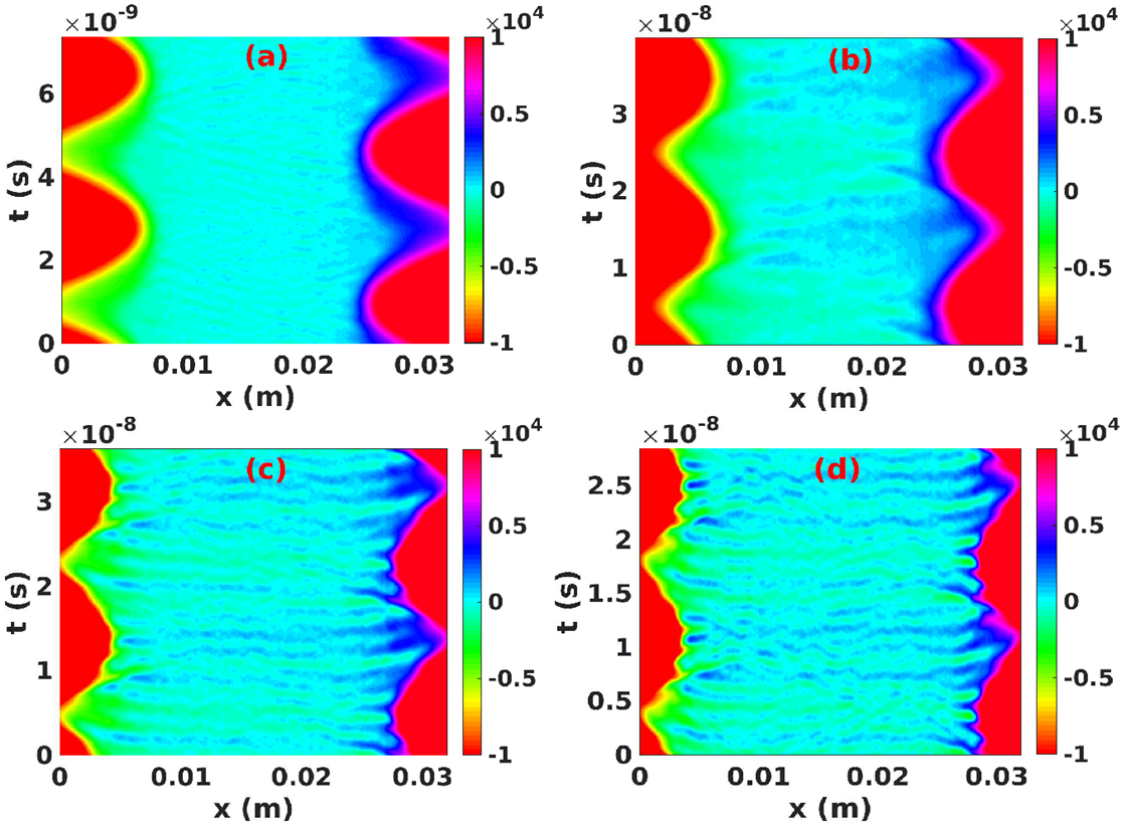

FIG. 3. Spatio-temporal evolution of electric field in the discharge at a) 27.12MHz b) 50MHz c) 55MHz and d) 70MHz driving frequency for constant driving voltage, 100V.

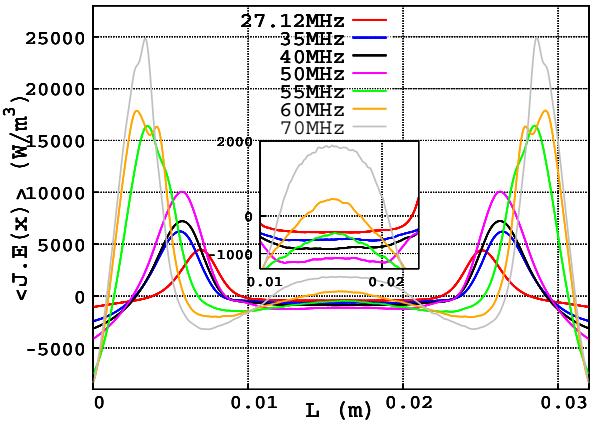

FIG.4. Average plasma heating (<J.E>) in the discharge for different driving frequencies and for a constant driving voltage of 100V.

In summary, we have investigated the effect of driving frequency on the EEDF in a low pressure capacitively coupled plasma discharge at a constant driving voltage. We observed a transition in the EEDF from a strongly bi-Maxwellian at a driving frequency of 27.12 MHz, to a convex type at the transition frequency, 50 MHz, and thereafter a weak bi-Maxwellian at higher driving frequencies. The change in the EEDF leads to a two-fold increase in the effective electron temperature up to the transition frequency, whereas, the electron density remains unchanged during this transition. Above the transition frequency a rapid increase in the electron density is observed along with a positive <J.E> (at 60 and 70 MHz driving frequency) in the bulk plasma and a slight decrease in the electron temperature. The transition occurs simultaneously with the onset of strong bulk-plasma and sheath-edge electric field transients which is of the order of electron plasma frequency. These transient electric fields are described by a self-reinforcing interaction between polarization electric fields in the bulk plasma and enhanced electron-sheath interaction for bunched, energetic electron currents. This observation of bunched, energetic 'beams' dramatically alters the electric field shape at the sheath and could have significant impact on the understanding of non-collisional power transfer into plasma electrons.

This work was funded by the Korea Institute for the Advancement of Technology and Ministry of Knowledge Economy (L-2010-1438-000), Republic of Korea; and Enterprise Ireland CF 20144043, cofunded by the European Regional Development Fund (ERDF) under the National Strategic Reference Framework (NSRF) 2007–2013. IPR group is supported by Department of Science & Technology (DST), Government of India via Projects GITA/ DST/TWN/ P-56/ 2014, DST-JC Bose Fellowship and YOS Professor PKK 92-14.

[1]A. A. Howling, J. L. Dorier, C. Hollenstein, U. Kroll and F. Finger F, J. Vac. Sci. Technol. A **10**, 1080 (1992).

[2]M. Surendra M and D. B. Graves D B, Appl. Phys. Lett. **59**, 2091 (1991).

[3]E. Abdel-Fattah and H. Sugai, Jpn. J. Appl. Phys. **42**, 6569 (2003).

[4]E. Abdel-Fattah and H. Sugai, Appl. Phys. Lett. **83**, 1533 (2003).

[5]E. Abdel-Fattah, M. Bazavan and H. Sugai, Phys. Plasmas **19**, 113503 (2012).

[6]E. Abdel-Fattah and H. Sugai, Phys. Plasmas **20**, 023501 (2013).

[7]H. Takekida and K. Nanbu, Jpn. J. Appl. Phys. **43**, 3590 (2004).

[8]C. K. Birdsall, *Plasma physics via computer simulation* (Adam Hilger, Bristol, 1991).

[9]R. W. Hockney and J. W. Eastwood, *Computer simulation using particles* (Adam Hilger, Bristol, 1988).

[10] M. M. Turner, A. Derzsi, Z. Donkó, D. Eremin and S. J. Kelly, Phys. Plasmas 20, 013507 (2013).

[11]V. A. Godyak and R. B. Piejak, Phy. Rev. Lett. **65**, 996 (1990).

[12]T. Gans, J. Schulze, D. O'Connell, U. Czarnetzki, R. Faulkner, A. R. Ellingboe and M. M. Turner, Appl. Phys. Lett. **89**, 261502 (2006).

[13]J. Schulze, T. Gans, D. O'Connell, U. Czarnetzki, A. R. Ellingboe and M. M. Turner, J. Phys. D: Appl. Phys. **40**, 7008 (2007).

[14] S. Wilczek, J. Trieschmann, J. Schulze, E. Schuengel, R. P. Brinkmann, A. Derzsi, I. Korolov, Z. Donko and T. Mussenbrock, Plasma Sources Sci. Technol. **24**, 024002 (2015).

[15]I. D. Kaganovich, O. V. Polomarov and C. E. Theodosiou, IEEE Trans. Plasma Sci. **34**, 696 (2006).

[16]S. Sharma, S. K. Mishra and P. K. Kaw, Phys. Plasmas **21**, 073511 (2014).

[17]S. Sharma, S. K. Mishra, P. K. Kaw, M. M. Turner and S. K. Karkari, Contrib. Plasma Phys. **55**, 331 (2015).

[18]M. Surendra M and D. B. Graves D B, Phys. Rev. Lett. **66**, 1469 (1991).

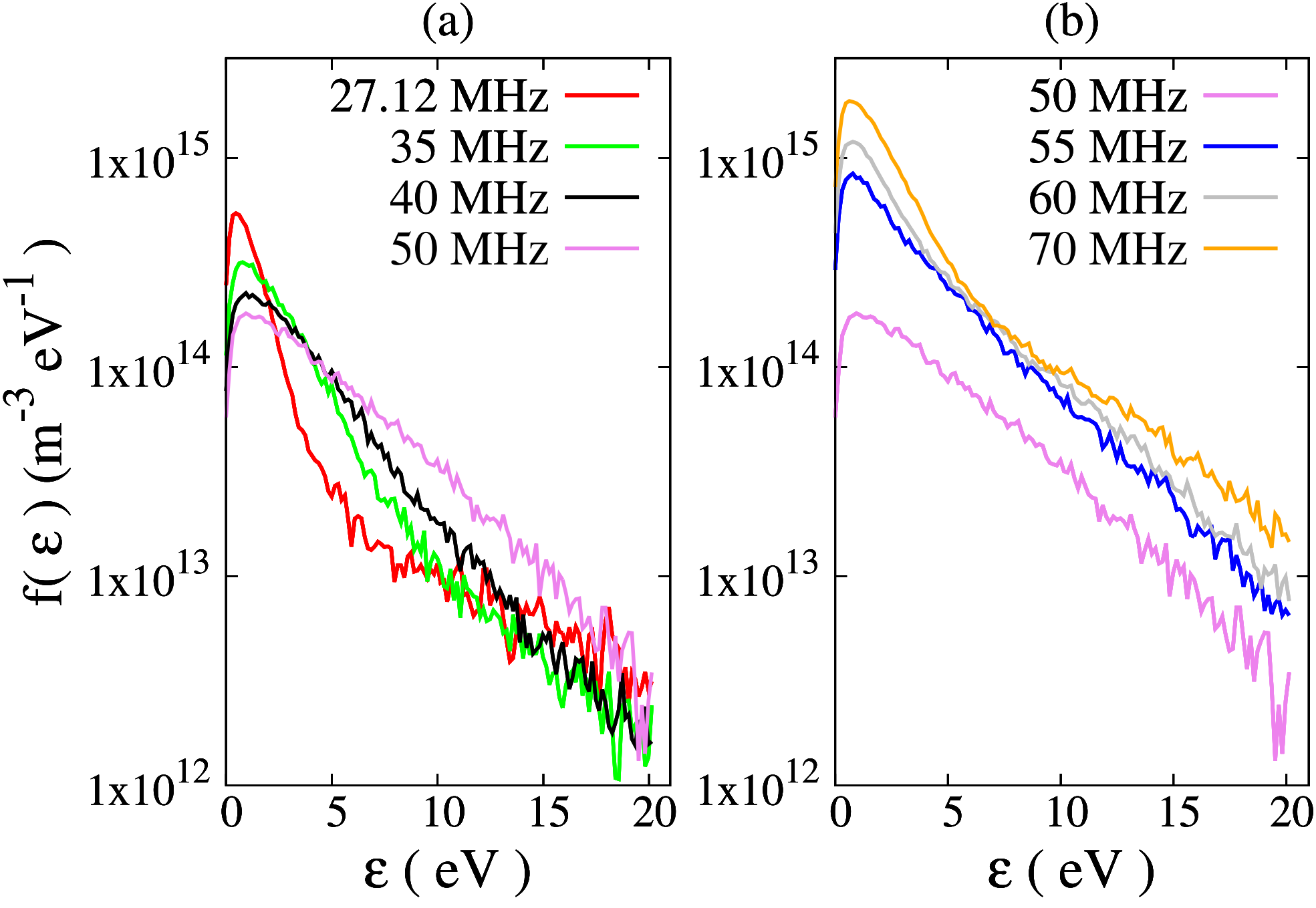
(a)
(b)
27.12 MHz
35 MHz
40 MHz
50 MHz
50 MHz
55 MHz
60 MHz
70 MHz
1x10^15
1x10^14
1x10^13
1x10^12
f(ε) (m^-3 eV^-1)
0
5
10
15
20
ε (eV)

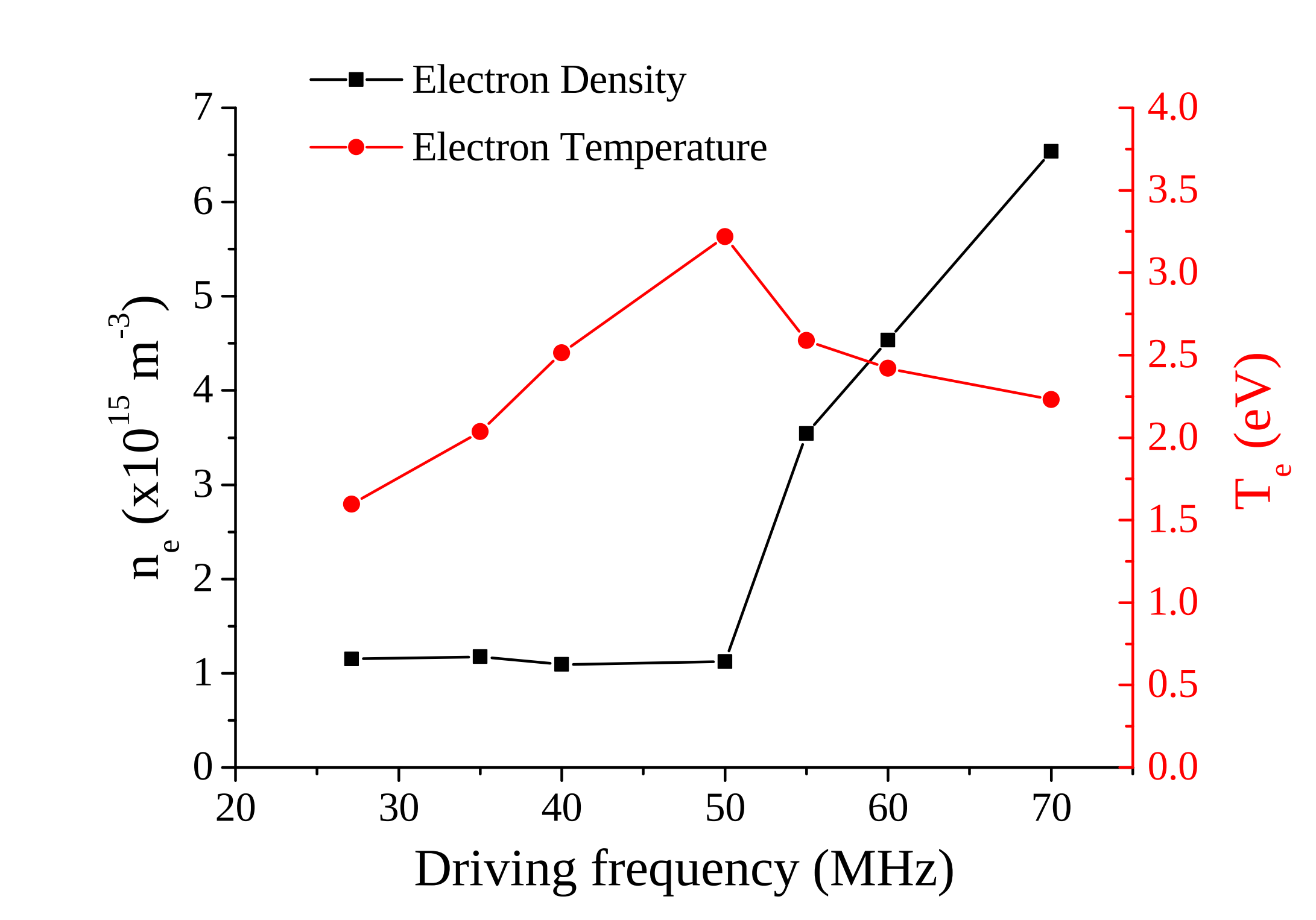
Electron Density
Electron Temperature
n_e (x10^{15} m^{-3})
T_e (eV)
Driving frequency (MHz)
0
1
2
3
4
5
6
7
0.0
0.5
1.0
1.5
2.0
2.5
3.0
3.5
4.0
20
30
40
50
60
70

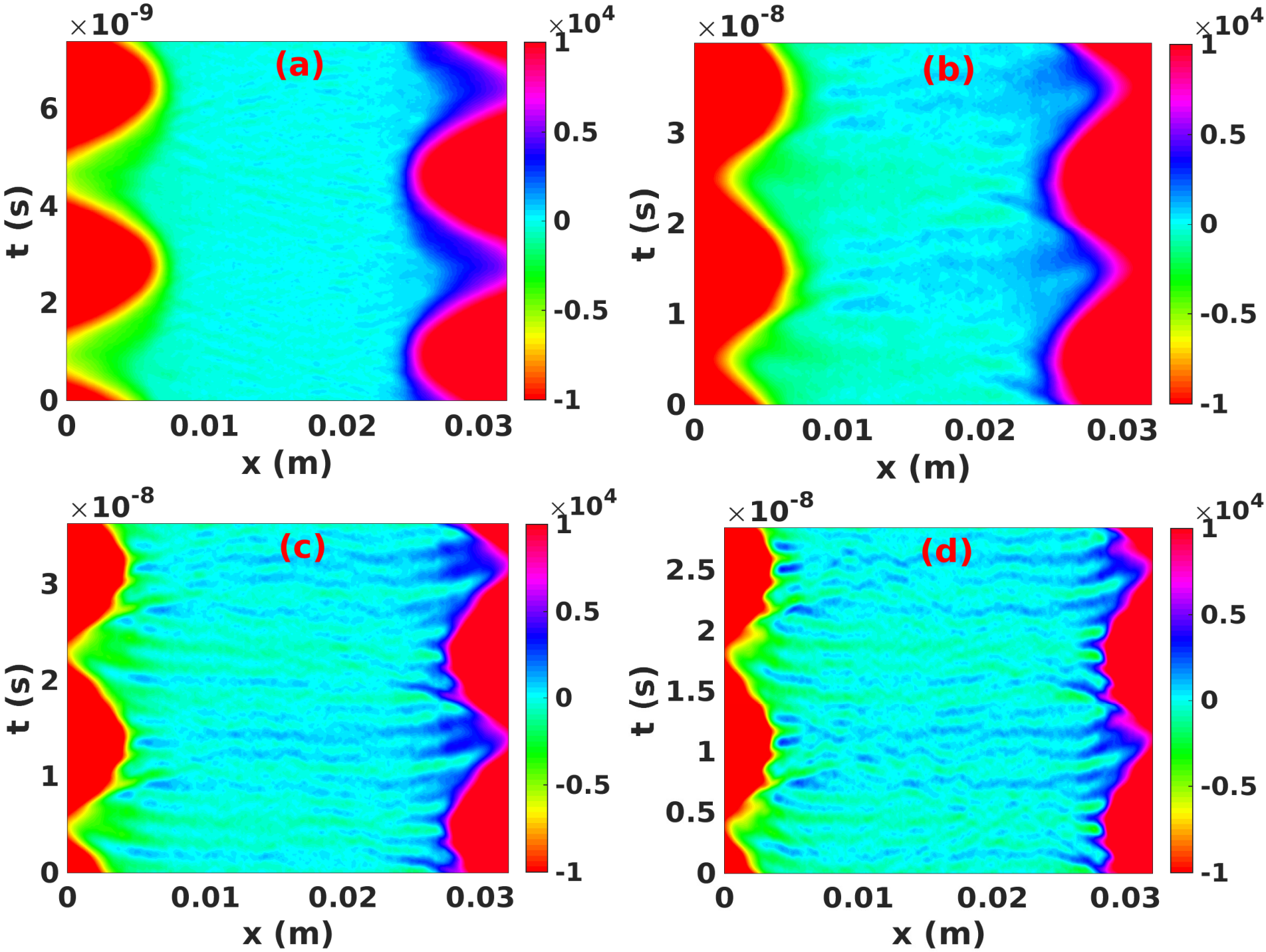
(a)
(b)
(c)
(d)
×10^-9
×10^-8
×10^4
t (s)
x (m)
0
0.01
0.02
0.03
0.5
-0.5
-1

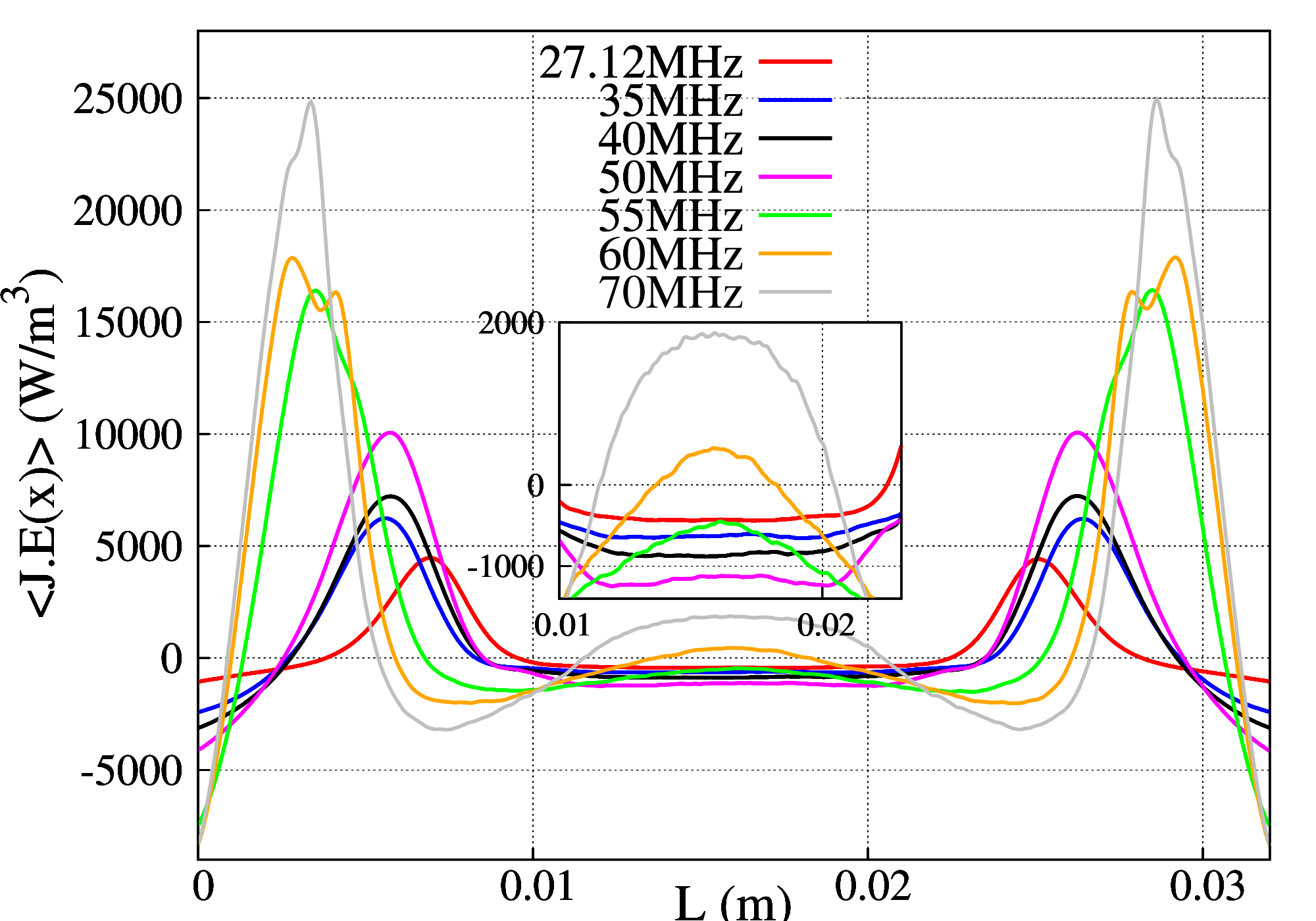
27.12MHz
35MHz
40MHz
50MHz
55MHz
60MHz
70MHz
25000
20000
15000
10000
5000
0
-5000
<J.E(x)> (W/m3)
2000
0
-1000
0.01
0.02
0
0.01
0.02
0.03
L (m)